

THE MUNICH HEAVY ION POST ACCELERATOR

E. Nolte, G. Geschonke, K. Berdermann, R. Oberschmid, R. Zierl,
M. Feil, A. Jahnke, H. Morinaga
Fachbereich Physik, E17, Techn. Universität München, Germany

Summary

The post accelerator in the Munich MP-tandem laboratory is a linear radio-frequency accelerator of the Interdigital-H-structure (IH). This structure has a particular high shunt impedance for particle velocities in the range $0.05 < \beta < 0.10$. In this velocity range the effective shunt impedance is empirically well described by $Z_{\text{eff}} = 13(\pm 1) \text{ M}\Omega/\text{m} \cdot \beta^{-0.84}$. The drift tube configuration is changeable in order to adjust the structure to the different particle velocities of the ion beams from the tandem accelerator. The eigenfrequency of different configurations varies between 55 and 80 MHz. With an applied rf-power of 50 kW in continuous operation it is possible, to increase the energy of the ion beam by a factor of 1.5-2. Acceleration tests have been performed with α -particles from a radioactive ^{241}Am α -source. The α -particles were accelerated with 50 kW rf-power from 4.1 MeV to 14.9 MeV. A beam of ^{32}S ions from the tandem with charge state 14+ was accelerated from 100 MeV to 160 MeV with an applied rf-power of 40 kW.

Interdigital-H-(IH) Structure

Principle of operation

For the postaccelerator at the Munich MP-tandem laboratory an Interdigital-H-structure (IH) has been chosen. This structure has been studied by H. Morinaga [1], J. Pottier [2], J.P. Blewett [3], V.A. Bomko et al. [4], P.M. Zeidlitz et al. [5], and M. Bres et al. [6]. In this accelerator type the ions pass a cylindrical cavity in axial direction. Drift tubes are fixed electrically conductive alternately at two opposite sides of the cavity. By exciting the resonator cavity in a H₁₁₁-mode, adjacent drift tubes are charged oppositely and the gap voltage can be used for particle acceleration.

Measurements of shuntimpedance and frequency on the model

In order to investigate the shuntimpedance and the resonance frequency of our IH-structure in dependance of the period length L and the relative gap width g/L, systematic measurements were done on a 1 : 3.3 model. In these measurements idealized drift tube configurations with $L = \text{const}$ and $g/L = \text{const}$ over the accelerator length were used. Measurements show, that the results can be used for real accelerating structures, when average values for L and g/L are used. The results of these measurements, extrapolated to the original accelerator size, are shown in fig. 1 and fig. 2. It is seen, that the frequency decreases with increasing capacitance between the drift tubes. This capacitance increases with decreasing gap length and increasing number of drift tubes. Operating frequencies for the

considered velocity range of the ions lie between 55 and 80 MHz. The effective shuntimpedance decreases with increasing particle velocity mainly because of the smaller number of accelerating gaps. For a given particle velocity the effective shuntimpedance is maximum for $g/L = 0.5$. For this value of g/L the effective shuntimpedance is empirically well described by $Z_{\text{eff}} = 13(\pm 1) \text{ M}\Omega/\text{m} \cdot \beta^{-0.84}$. For a typical velocity of $\beta = 8.8\%$ and a rf-power input of 50 kW a total accelerating voltage of 5 MV is obtained. Fig. 3 shows the measured values of the effective shuntimpedance for $g/L = 0.5$ in comparison with other accelerating structures, which are used in this velocity range, as Wideroe-, Alvarez- and Helix-accelerators.

Construction of the Cavity

The cavity is constructed as vacuum tank. Fig. 4 shows its design. The total length is 5 m, the diameter 1 m. Drift tubes are mounted over a length of 4 m. The tank is manufactured of 10 mm thick steel and consists of 3 parts, each of which is watercooled. All inner surfaces are electrolytically copper plated. The copper is 0.3 mm thick with a surface roughness of 3 μm . The drift tubes have no separate cooling, they are made of solid copper and are fixed to the watercooled middle part. The drift tube configuration can be changed easily when the tank is opened. Vacuum- and rf-seal is a pure Al-wire. With a 1100 l/sec turbomolecular pump the vacuum without rf-power is 10^{-7} torr, with an applied rf-power of 50 kW it is 10^{-6} torr.

Rf-System

The resonance frequency of the cavity depends on the chosen drift tube configuration and lies in the range of 55-80 MHz. Therefore, the rf power supply has been constructed tunable from 50-100 MHz. The rf-power source is a transmitter-amplifier with 50 kW output power in continuous operation. It consists of a crystal controlled frequency synthesizer, 100 W broad band amplifier

5 kW driver stage

50 kW power stage

The last two stages are grounded grid amplifiers with RCA 8793 and Siemens RS 2052 J power tetrodes, respectively. They are tunable by means of coaxial line resonators with variable length. Inputs and outputs of all stages are matched to 50 Ω transmission cables. The rf-power is coupled inductively into the tank. The coupling loop is sealed to the vacuum by a ceramic vase. The resonance frequency of the tank is controlled by means of a copper cylinder with 6 l volume, which can be moved parallel to the cavity axis near the wall onto places of different magnetic field strength. Thus a relative frequency drift of the accelerator cavity of 10^{-3} can be compensated. The control signal is de-

duced from the phase angle between the in-coupled rf and a signal coupled out of the tank.

Beam Line System

Fig. 5 shows the position of the post accelerator in the beam line system of the Munich accelerator laboratory. After the tandem the ions pass a post stripper. In the 90° deflection magnet the beam is analysed. In order to increase the intensity of the postaccelerated beam, a rf-buncher will be installed after the switching magnet 20 m before the post accelerator. This buncher is constructed as coaxial $\lambda/4$ resonator, which can be tuned to the frequency of the post accelerator between 50 and 100 MHz. Two target places are provided for the postaccelerated beams: one in the focal plane of the quadrupole lens behind the post accelerator and one in the focal plane of an analysing system consisting of two left-turning 90° magnets and a quadrupole singlett in the symmetry plane between them. The calculated energy resolution of the beam analysed by slits in the symmetry plane is $4 \cdot 10^{-4}$, the maximum energy window is $5 \cdot 10^{-2}$.

Beam Dynamics

Our accelerating structure is short, because a) the energy gain is smaller than the input energy of the ions and b) the captured ions perform less than $1/3$ phase oscillations. This means, that the radial defocussing is small (a) and the usable phase acceptance for acceleration includes also non-captures ions (b). So, even at a synchronous phase of 0° the usable range is still finite. In this case the radial defocussing action can be neglected. Therefore, no radial focussing elements are needed inside the tank. So, construction and installation of the drift tubes are very simple and the drift tube configuration can be changed easily. By means of quadrupole doublets located before and after the tank, the beam can be matched to the acceptance of the post accelerator and focussed onto the target. Calculations show, that for a synchronous phase of 0° 17% of the beam intensity can be used for acceleration. With the buncher 56% of the tandem beam are accelerated. Rf-buncher and post accelerator (frequency f) can be synchronized with the pulsing system of the tandem (frequency $f/16$), which consists of chopper and prebuncher between ion source and tandem. In this case 100% of the ion beam from the tandem can be accelerated. The pulse length of the postaccelerated beam at the target 4 m behind the post accelerator will then be ~ 120 psec.

Post Acceleration of Tandem Beams

Table 1 shows the calculated beam energies of the tandem and the post accelerator. For this calculation a tandem voltage of 12.5 MV, the measured shuntimpedances, the most probable charge states q_T and q_P of the terminal- and post-stripper and the charge states q_{T+2} and q_{P+2} are used. In addition some Coulomb barriers are also listed. It is thus possible to bombard any target with S or Ca at beam energies above the Coulomb barrier.

Particle Acceleration Experiments

Acceleration of α -particles

The post accelerator was tested by accelerating α -particles from a $1\text{mCi } ^{241}\text{Am-}\alpha$ -source with a rf-power input up to 50 kW. The α -emission spectrum is peaked around 4.09 MeV with a FWHM=510 keV. The energy of the accelerated α -particles was measured with a Si surface-barrier-detector. In a drift tube configuration built for a rf-power input of 3 kW and synchronous phase of 0° the α -particles were accelerated from 4.09 MeV to 7.3 MeV. From this an effective shuntimpedance of $170 \text{ M } \Omega/\text{m}$ is calculated. Fig. 6 shows the energy spectrum of accelerated α -particles for a rf-power input of 50 kW and a synchronous phase of 0° . The experimental setup was: α -source-post accelerator-magnetic quadrupole doublet-Si surface-barrier-detector. With the quadrupole doublet the particles with high energies were focussed on the detector. The α -particles were accelerated from 4.09 MeV to 14.9 MeV, which corresponds to a total tank voltage of 5.4 MV and an effective shuntimpedance of $117 \text{ M } \Omega/\text{m}$.

Acceleration of a ^{32}S Beam

A first test with a 100 MeV ^{32}S -beam from the tandem accelerator was performed. In the post-stripper a charge state of $14+$ was produced and analysed with the 90° -magnet. The drift tube configuration for this measurements was built for rf-power input of 40 kW and a synchronous phase of 0° . The accelerated particles were focussed with the quadrupole lens after the post accelerator on a $520 \mu\text{g}/\text{cm}^2$ gold foil. At 20° to the beam axis the Rutherford-scattered ions were detected with a Si-surface-barrier-detector. The measured energy spectrum is shown in fig. 7. The S-ions were accelerated from 100 MeV up to 160 MeV, which corresponds to a total tank voltage of 4.3 MeV and an effective shuntimpedance of $92 \text{ M } \Omega/\text{m}$.

References

1. H. Morinaga: Japan.Phys.Soc. Meeting, Osaka 1949
2. J. Pottier: IEEE Trans.Nucl.Sci. NS-16, No.3 (1968)552
3. J.P. Blewett: CERN Symposium, 1,161 (1956)
4. V.A. Bomko, E.I. Revutshii: Sov.Phys-Techn. Phys. Vol. 9, No.7 (1965)973
5. P.M. Zeidlitz, V.A. Yamnitzki: Plasma Physics 4 (1962)121
6. M. Bres, A. Chabert, F. Foret, D.T. Tran, G. Voisin: Part.Acc. 2 (1971)17

Beam	Tandem Energy [MeV] for q_T	Final Energies [MeV] for		Coulomb Barrier (lab.) [MeV]
		q_T, q_p	q_T+2, q_p+2	
^{32}S	125	192	226	$\text{S} \rightarrow \text{Pu}$: 184
^{40}Ca	137.5	220	255	$\text{Ca} \rightarrow \text{Pu}$: 234
^{58}Ni	137.5	247	287	$\text{Ni} \rightarrow \text{Sm}$: 270
^{79}Br	150	282	323	$\text{Br} \rightarrow \text{Br}$: 286

Tab. 1: Energies of some typical beams after the tandem and after post acceleration with 50 kW rf-power.

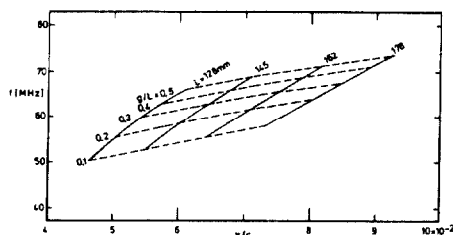


Fig. 1. Frequency of drift-tube configurations with different period lengths L and gap-/period-lengths g/L in dependence of the particle velocity $\beta = v/c$ measured on the 1:3.3 model, converted to the original accelerator.

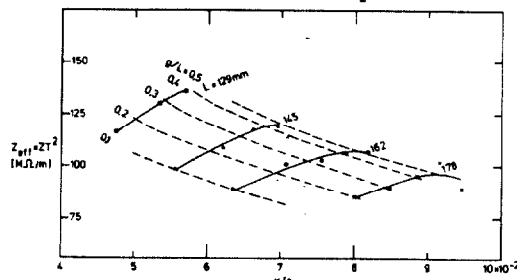


Fig. 2. Effective shunt impedance as a function of the particle velocity. The varied parameters are the periodic length L and the relative gap width g/L .

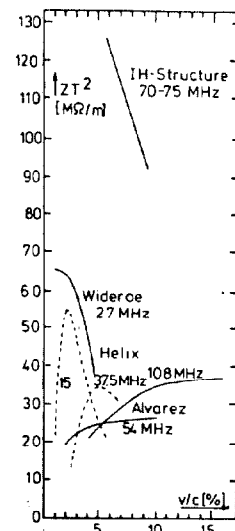


Fig. 3. Effective shunt impedance of accelerating structures in dependence of the particle velocity.

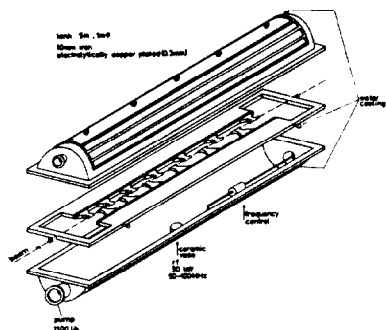


Fig. 4. Construction of the post accelerator tank.

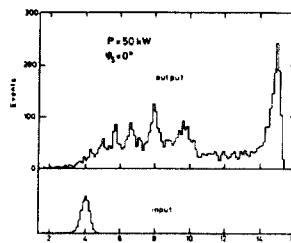


Fig. 6. Energy spectrum of post-accelerated α -particles (input energy = 4.09 MeV, $\phi_s = 0^\circ$, $P_{RF} = 50 \text{ kW}$).

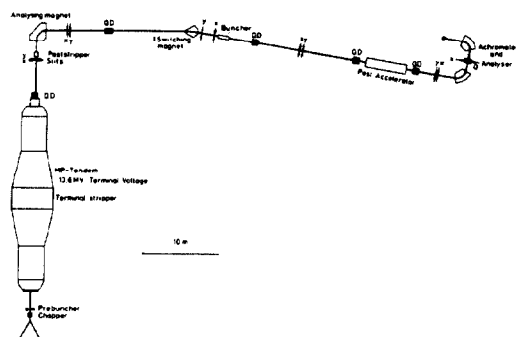


Fig. 5. Position of the post accelerator in the Munich MP-tandem laboratory.

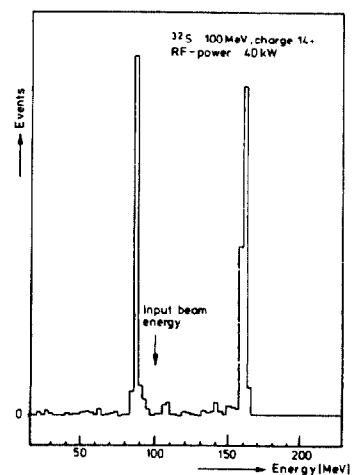


Fig. 7. Energy spectrum of a post-accelerated ^{32}S beam (input energy = 100 MeV, $\phi_s = 0^\circ$, $P_{RF} = 40 \text{ kW}$).